Title	Peeling of Carbon Nanotubes during Tensile Failure in Al Matrix Composites
Author(s)	Chen, Biao; Li, Shufeng; Imai, Hisashi et al.
Citation	Transactions of JWRI. 2014, 43(1), p. 29-32
Version Type	VoR
URL	https://doi.org/10.18910/50960
rights	
Note	

Peeling of Carbon Nanotubes during Tensile Failure in Al Matrix Composites†

CHEN Biao*, LI Shufeng, IMAI Hasashi, JIA Lei, UMEDA Junko, TAKAHASHI Makoto, and KONDOH Katsuyoshi**

Abstract

In-situ scanning electron microscopy (SEM) observation of a tensile test was performed to investigate the fracturing behaviour of multi-walled carbon nanotubes (MWCNTs) in powder metallurgy Al matrix composites (AMCs). A peeling phenomenon during MWCNT fracturing was clearly observed, and its formation mechanism was examined. During tensile failure, CNT defects having a local weak strength resulted in the axial shift of wall-breaking positions and the following inter-wall sliding. Peeling behavior and resultant morphology of peeled CNT were dependent on structure and distribution of the defects inside CNTs. These results provide new understandings of the fracturing mechanisms of CNT reinforcements for designing high-performance metal matrix composites.

KEY WORDS: (Metal matrix composites), (Carbon nanotubes), (Aluminum), (Fracture), (Peeling)

1. Introduction

Carbon nanotubes (CNTs), due to their unique one or multi-layer tubular graphene structure, have attracted great attention for structural and functional uses.[1)] Excellent mechanical properties, high aspect ratio, large surface area and light weight, make CNTs ideal fibrous reinforcements for composites materials. In the last decade, CNT-reinforced metal matrix composites (MMCs) have been studied intensively for applications as the next generation of strong and lightweight structural materials in aerospace and automotive industries.[2)] Up to date, however, the reported mechanical properties of CNT reinforced metal matrix composites (MMCs) are much lower than expected. The understanding of the strengthening effect of CNT is basically essential to the design of high-strength MMCs.[2-6)] Its concentrated topic is the fracturing behavior of CNTs in composites, which provides incisive and detailed information on the mechanical response of CNTs during composite failure.

The fracturing behavior of multi-walled CNTs (MWCNT) outside composites has been investigated by in-situ scanning electron microscopy (SEM) observations.[7, 8)] Individual CNTs were loaded on two atomic force microscopy (AFM) cantilever probes. CNT was observed in a 'sword-in-sheath' failure mode: the outermost wall of MWCNT was fractured and the inner walls were pulled out. Different from this situation, during the fracturing of CNT reinforced composites, CNTs were loaded by the surrounding matrix or interfacial phases. Moreover, wetting conditions and probably happened reactions at interfaces will influence the interface bonding strength. Even severe interface reaction between CNTs and metal matrices at high processing temperatures would cause structure change of CNTs. These facts might result in quite different mechanical behaviours of CNTs during composite failure. Therefore, the fracturing behavior of CNTs in MMCs should be reconsidered and intensively investigated for the design of high-strength MMCs. In this study, MWCNT-reinforced pure Al matrix composite was fabricated by a powder metallurgy process, and an in-situ scanning electron microscopy (SEM) observation of tensile CNTs/Al composite was applied to examine the CNT fracturing behavior during CNTs/Al composite failure. Peeling fracturing behaviours were detected from the in-situ SEM observations. The possible formation reason was discussed from the viewpoint of load transfer between matrix and CNTs, and between adjacent CNT walls.

2. Experimental methods

The CNTs/Al composite was fabricated through a powder metallurgy route. Pure Al and MWCNT (commercially named VGCF-H, 0.6 wt.%) powders were mixed by Al_2O_3 media balls (ball to powder massive ratio

† Received on June 30, 2014
* Graduate Student
** Professor

Transactions of JWRI is published by Joining and Welding Research Institute, Osaka University, Ibaraki, Osaka 567-0047, Japan

of 1:10) using a rocking milling machine (Seiwa Giken) for 4 h. The milled powder mixture was subsequently consolidated by sparking plasma sintering (SPS) and the following hot-extrusion. SPS was conducted by using an SPS system (SPS-1030S, SPS Syntex) at a sintering temperature of 823 K held for 0.5 h at a pressure of 30 MPa under a vacuum of 5 Pa. Before hot extrusion, the as-sintered billet was preheated at 773 K for 180 s under an argon gas atmosphere. The billet was then immediately extruded using a 2000 kN hydraulic press machine (SHP-200-450, Shibayama). The extrusion ratio and the ram speed were 12:1 and 0.5 mm/s, respectively. The morphologies of raw CNT and the extruded CNT/Al composites were examined by transmission electron microscopy (TEM, JEM-2010, JEOL). TEM samples of the composites were fabricated with a focused ion beam (FIB, HITACHI FB-2000A) system.

The in-situ tensile test of CNTs/Al composite was operated inside a field emission SEM (FE-SEM, JEM-6500F, JEOL), as shown in **Figure 1**. The sample was machined from the extrusion rod into a flat dog-bone shape with gauge length of 10 mm. The effective cross-section area is 2 mm in width and 1 mm in thickness, as shown in the inset of Fig. 1a. The sample was placed into the two clamping heads of the tensile machine, and then loaded with a tensile speed of 5 μm/s. Tensile test was manually paused during the tensile test, and the curve obtained from the load as a function of displacement as shown in Fig. 1b. During the pause (stage a through e in Fig. 1b), the load and displacement were held on and SEM photos were captured. Tensile loading was then restarted to the next pause point until the sample was fractured (stage f). In order to control the fracturing position, the tensile sample was pre-treated by cutting two notches on the middle position and a groove between them on the as-machined sample (inset of Fig. 1b).

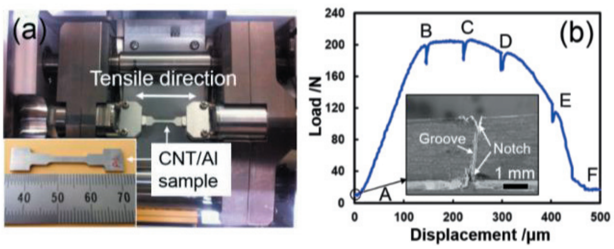

Fig. 1 Tensile stage placed in SEM (a) and recorded load-displacement curve for in-situ observation of CNT/Al composite during the tensile test (b).

3. Results and discussion

Figure 2 shows the TEM observations of raw MWCNT at different magnifications. CNT exhibited a large aspect ratio (length to diameter ratio) over 100. Structure defects were observed in CNT (as arrows indicated in Fig. 2b). The high-resolution TEM (HRTEM) image (Fig. 2c) clearly shows the morphology of some typical defects. CNT defects destroyed the complete wall structure and even caused nano-pores (Fig. 2c), which will undoubtedly affect the strength distribution on the CNT walls. However, it is known that defects are hard to prevent in MWCNT. Especially, the commonly used CVD-grown MWCNT has a high defect density.[9)]

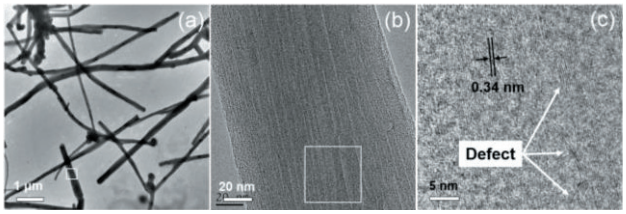

Fig. 2 Morphology of raw MWCNT by TEM observations at different magnifications. (b) shows the box in (a). (c) shows the box in (b).

Figure 3 shows the morphology of MWCNT in AMCs. CNT is well contacted with Al matrix via a clean interface, and no other interface phases could be observed (Fig. 3a). Moreover, CNT walls are largely preserved from raw materials (Fig. 2) to composite (Fig. 3b). These results suggest that CNTs are stable in the present processing conditions. As a result, the defects inside CNTs also remained IN the composite. The frame in Fig. 3b shows a typical defect consisting of about 30 walls. The walls were non-parallel to the axis direction and cross-lined with other walls.

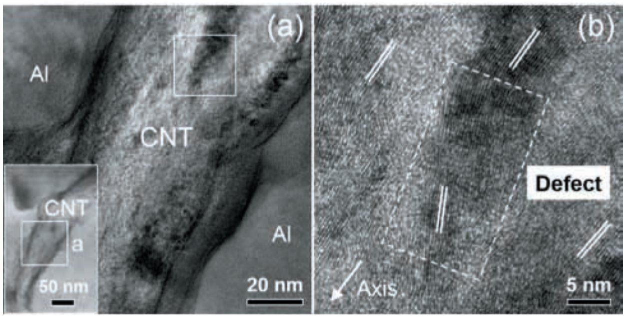

Fig. 3 Morphology of MWCNT dispersed in AMCs by TEM observation at different magnifications. (b) shows the box in (a). Double-lines in (b) suggest the aligning direction of walls.

The fracturing of MWCNT in AMCs in different tensile test stages is shown in **Figure 4**. Each photo (Fig. 4a through f) is corresponding to the stage given the corresponding capital letter (A through F) in Fig. 1b. From the starting stage (Fig. 4a) to the end of yielding stage (Fig. 4b), little microstructure change of the composite could be observed. MWCNTs were still buried in the composite. From stage B to C (Fig. 2b), plastic deformation started, and then micro-cracks occurred and grew in the sample (Fig. 3c). As the crack expanded, CNTs were exposed and restrained the growing tendency of the crack. As the tensile displacement was increased, CNTs began to fracture one by one (Fig. 3d). The outer walls of the CNT designated as ① has fractured and some debris is touched on the broken area. The fresh inner nanotube of CNT ① is exposed with a decreased out-diameter as an arrow indicated in Fig. 3d. Spontaneously, CNT ② is experiencing a peeling fracture process with multi-fractured-stages. From the diameter gradient of the left CNT segment, it suggests that, like CNT ①, CNT ② initially fractured at the outer layer, and the wall-breaking vertically grew into the CNT with some depth. Then the fracturing position shifted to another position some axial distance away from the start point. This peeling behavior has repeated twice along the tensile direction, leaving 3 rod stages with different out-diameters. The arrows with different lengths indicate the consequent wall-breaking. The peeling behavior will move on until all the walls are fractured. In Fig. 3e and f, CNTs are completely peeled and exhibited with distinct stages with different diameters. The peeling consequently happened, exhibiting gradient varied tube diameter. The positions of vertical wall-breaking are shown as arrows indicated in Fig. 4d through f.

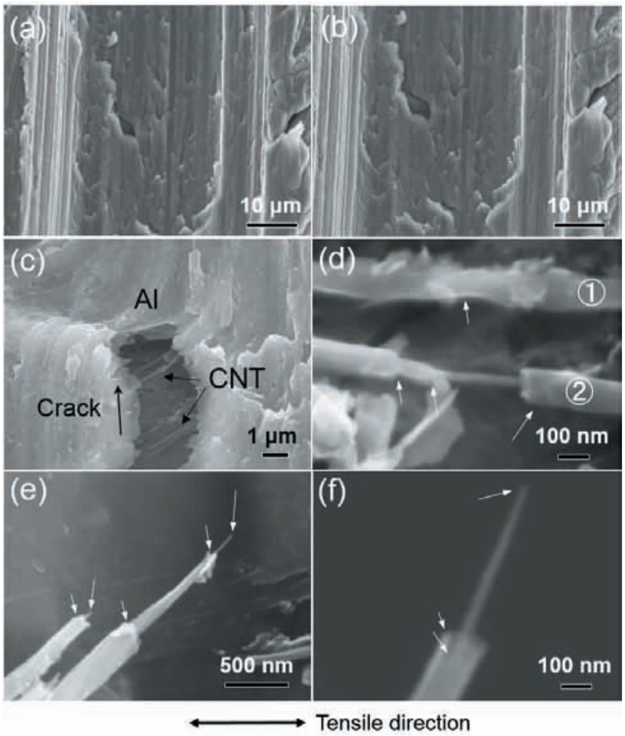

Fig. 4 In-situ SEM observations of CNT during different processes in tensile test. (a) through (f) are corresponding to the states in Fig. 1b. White arrows in (d) through (f) indicate the positions of vertical wall-breaking. Longer arrows suggests the later happened breaking for each CNT.

Because of the effectively metallurgical bonding between the outermost wall of CNTs and the matrix Al (Fig. 3a), a shear stress can be formed and help to transfer load to the outermost wall during composite failure.[10] If the CNT-Al interface is strong enough, tensile stress applied in the outermost wall will reach the strength of the wall, i.e., CNTs begin to fracture from the outermost wall (CNT ① in Fig. 3d). As the displacement increases after the outer wall breaks, the load will be probably transferred to the inner wall through van der Waals (vdW) force, also in the form of shear stress.[11] Although inter-wall shear resistance (ISR) resulting from vdW force is weak in a perfect CNT [11, 12], it might be greatly enhanced by the cross-linking of defect walls (Fig. 3b) and the compressive stress applied on CNT during consolidation.[13] Therefore, stress is produced on the wall to balance the shear stress from the inner adjacent wall and the outer one. To simply examine the tensile stress distribution on the walls, as Kelly suggested [10], assume that stress at the wall ends are 0, and at a given time, the shear stress between two adjacent walls is a constant value at any wall position. The stress distribution of a wall along the axis direction can be expressed as:

$$\sigma(x, i) = \frac{|\mathrm{L}-2x|}{2\mathrm{d}} \cdot (\tau_{i-1} - \tau_i) \qquad \text{(Eq. 1)}$$

where x is the position away from the CNT center, i (=1, 2, …) is the ordinal number of the wall countered from outside, L is the length of the wall or the CNT, d is the thickness of the wall, and τ_i is the shear stress between i-wall and (i+1)-wall. Especially, $\tau 0$ means the shear stress between the matrix and the outermost wall. The stress distribution of a wall in breakage is schematically illustrated in Fig. 5. From the relation between $\sigma(x, i)$ and x, it is clear that the center point (x=0) always has the maximum stress. It means, if the CNT wall is perfect or strength distribution of the wall $\sigma_{CNT}(x, i)$ is a constant, and τi-1 is large enough, $\sigma(0, i)$ tend to first reaches the CNT strength, and wall breaks up at the center, resulting in $\sigma_p(x, i)$ (Fig. 5). However, the existence of defects inside CNT makes different results in fact. At the defect point, $\sigma_{CNT}(x, i)$ will become much smaller. If several defects exist on the same wall, suppose the point x=xi first reaches the wall strength, it becomes the weak point of the wall so that the wall will break there, resulting in $\sigma_d(x, i)$ (Fig. 5). This means, during CNT fracturing, the wall-breaking point probably shifts to another position with some axial distance, exhibiting the peeling behavior. At the same time, a crack slides to the weak point inside CNT. When the breaking point shifts twice during failure, CNT will peel twice, forming 3 distinct gradient tubes (Fig. 4e and f), as schematically shown in Fig. 5. From a viewpoint of repeated peeling behavior, the reported 'sword-in-sheath' failure mode of the outermost wall [7] or layer [13, 14], is the simplest case that a small quantity of CNT walls peeled for one time. The preconditions of multiple peeling phenomena are i) a strong CNT-Al interface, ii) strong ISR to effectively transfer load between CNT walls, and iii) randomly dispersed wall defects. The peeling position was the result of competition of the size and morphology of various defects. Peeling times were related to the distribution of defects. Therefore, peeling behaviour and resulting fracture morphology of MWCNT are mainly dependent on the morphology and distribution of the defects. As peeling time is increased, the number of fracturing walls increases, so higher load can be transferred to CNT from the matrix and it can result in higher composite strength. Moreover, with the increase of peeling time, the crack length inside CNT may be greatly increased, which will result in remarkable toughness improvement of CNT-reinforced composites.[14] These results suggest CNT has high load-bearing capability in MMCs processed under proper conditions, which would fulfill the reinforcing potential for next-generation strong and light MMCs.

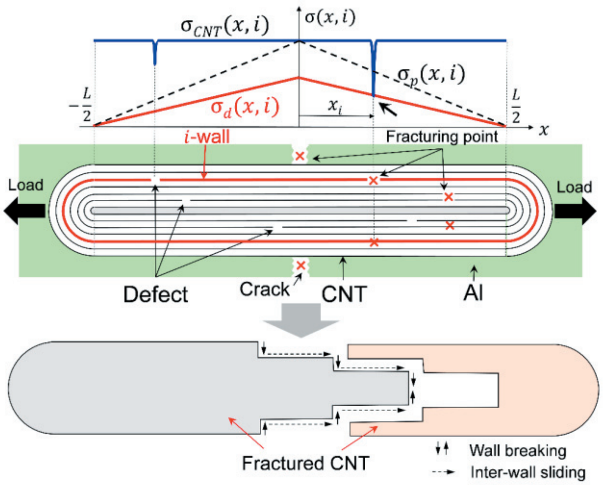

Fig. 5 Scheme of stress distribution on a wall of MWCNT and the peeling fracture mode of MWCNT during tensile failure.

4. Conclusion

In summary, an in-situ SEM observation of CNTs/Al composite was successfully applied to investigate the fracturing behavior of MWCNTs during tensile failure. A peeling phenomenon was commonly observed during the tensile test. During peeling, CNT defects were responsible for the axial shift of wall-breaking positions and inter-wall sliding. Fracturing behaviour and resultant fracturing morphology of MWCNT were greatly dependent on structure and distribution of the defects. Peeling phenomena showed relations with the mechanical response of composite during tensile failure. It might provide news insight into understanding the strengthening effect of CNT reinforcements in MMCs for designing high-performance materials.

References

1) V. N. Popov: "Carbon nanotubes: properties and application", Mater. Sci. Eng. R, 43-3, (2004), 61-102.
2) S. R. Bakshi, D. Lahiri and A. Agarwal: "Carbon nanotube reinforced metal matrix composites - a review", Inter. Mater. Rev., 55, (2010), 41-64.
3) S. R. Bakshi and A. Agarwal: "An analysis of the factors affecting strengthening in carbon nanotube reinforced aluminum composites", Carbon, 49, (2011), 533-44.
4) A. Esawi and K. Morsi: "Dispersion of carbon nanotubes (CNTs) in aluminum powder", Compos. Part A, 38, (2007), 646-70.
5) C. He, N. Zhao, C. Shi, X. Du, J. Li, H. Li and Q. Cui: "An approach to obtaining homogeneously dispersed carbon nanotubes in al powders for preparing reinforced Al-matrix composites", Adv. Mater., 19, (2007), 1128-32.
6) L. Jiang, G. Fan, Z. Li, X. Kai, D. Zhang, Z. Chen, S. Humphries, G. Heness and W. Y. Yeung: "An approach to the uniform dispersion of a high volume fraction of carbon nanotubes in aluminum powder", Carbon, 49, (2011), 1965-71.
7) M. F. Yu, O. Lourie, M. J. Dyer, K. Moloni, T. F. Kelly and R. S. Ruoff: "Strength and breaking mechanism of multiwalled carbon nanotubes under tensile load", Science, 287, (2000), 637-40.
8) A. H. Barber, R. Andrews, L. S. Schadler and H. D. Wagner: "On the tensile strength distribution of multiwalled carbon nanotubes", Appl. Phys. Lett., 87 (2005), 203106-3
9) C. Meyer, C. Spudat, L. Houben and C. M. Schneider: "Defects induced on chemical vapour deposition carbon nanotubes during peapod synthesis on substrates", Nanotech, 20, (2009), 065603.
10) A. Kelly and T. R. Tyson: "Tensile properties of fiber-reinforced metals: copper/tungsten and copper/molybdenum", J. Mech. Phys. Solids, 13, (1965), 329-50.
11) J. Cumings and A. Zettl: "Low-friction nanoscale linear bearing realized from multiwall carbon nanotubes", Science, 289, (2000), 602-4.
12) R. Bacon: "Growth, structure, and properties of graphite whiskers", J. Appl. Phys., 31, (1959), 283-90.
13) M. Estili and A. Kawasaki: "Engineering strong intergraphene shear resistance in multi-walled carbon nanotubes and dramatic tensile improvements", Adv. Mater., 22, (2010), 607-10.
14) G. Yamamoto, K. Shirasu, T. Hashida, T. Takagi, J. W. Suk, J. An, R. D. Piner and R. S. Ruoff: "Nanotube fracture during the failure of carbon nanotube/alumina composites", Carbon, 49, (2011), 3709-16.